

## Limits of the Fractal Dimension for Irreversible Kinetic Aggregation of Gold Colloids

D. A. Weitz, J. S. Huang, M. Y. Lin,<sup>(a)</sup> and J. Sung

*Exxon Research and Engineering Company, Annandale, New Jersey 08801*

(Received 26 November 1984)

We show that there are two regimes of irreversible, kinetic aggregation of aqueous colloids, determined by the short-range interparticle potential, through its control of the sticking probability upon approach of two particles. Each regime has different rate-limiting physics, aggregation dynamics, and cluster-mass distributions, and results in clusters with different fractal dimensions. These results set limits on the fractal dimension,  $d_f$ , for gold aggregates of  $1.75 \leq d_f \leq 2.05 (\pm 0.05)$ .

PACS numbers: 64.60.Cn, 05.40.+j, 82.70.Dd

Kinetic growth processes have attracted considerable attention recently with the realization that scaling concepts may be applied to describe many features of the phenomena.<sup>1</sup> In particular, it has been recognized that the structure of the resulting clusters can be described as a fractal,<sup>2,3</sup> leading to a new understanding about both the kinetic growth mechanisms themselves, as well as the physical properties of the aggregates. These concepts have been successfully applied to experimental investigations of several aqueous colloid systems and the expected dilation symmetry of the aggregates has been observed.<sup>4-6</sup> However, the measured fractal dimensions,  $d_f$ , appear to vary considerably. This raises questions about the universality of the fractal dimension produced in these systems, as well as the possible effects of the short-range interparticle interactions on  $d_f$ . In this Letter, we show that there are two regimes of kinetic aggregation, determined by the short-range interparticle interactions which affect the sticking probability upon the approach of two particles. Each regime has different rate-limiting physics, different dynamics, and different mass-weighted cluster distributions. Furthermore, the resulting clusters possess different fractal dimensions, which characterize the physical mechanisms governing the kinetics of the aggregation in each regime. This is, we believe, the first attempt to relate the short-range interparticle interactions to the long-range dilation symmetry of the resulting aggregates. Furthermore, we argue that the two regimes of kinetics, as well as the fractal dimensions that result from each, represent the limits obtained in irreversible cluster-cluster aggregation.

We investigate aqueous gold colloids<sup>7</sup> which consist of very uniform particles with radius  $a = 7.5$  nm. The aggregation is initiated by addition of a small amount of pyridine which displaces the charged ions from the surface of the colloid. The rate of aggregation is directly controlled by the amount of pyridine added and can be varied over many orders of magnitude. Addition of sufficient pyridine results in rapid aggregation,<sup>8</sup> with a rate consistent with dynamics limited

solely by the Stokes diffusion of the aggregates. Both the dynamics of aggregation,<sup>9</sup> and the structures which result,<sup>4</sup> exhibit scaling behavior, with  $d_f = 1.75$ . Our emphasis here is the other limiting case, when a sufficiently small amount of pyridine is added so that the aggregation rate is decreased by many orders of magnitude.

We follow the dynamics of the aggregation by measuring the first cumulant of the autocorrelation function of the quasielastically scattered light.<sup>10</sup> From this, we obtain an effective hydrodynamic radius,  $R$ , characteristic of the distribution of the growing clusters.<sup>9</sup> While the exact value of  $R$  measured for the slow aggregation exhibits some dependence on the scattered wave vector,  $k$ , we find the same characteristic behavior of the time dependence for  $R$  at all values of  $k$  accessible with our apparatus ( $3.4 \leq k \leq 18.7 \mu\text{m}^{-1}$ ). Thus the value of  $R$  must be viewed as the size of a characteristic cluster which reflects the time evolution of the distribution of aggregates.<sup>11</sup> The exact value of  $R$  measured for a given distribution depends<sup>12</sup> on whether  $kR$  is greater than or less than 1; so our measurements are made at high  $k$ , where  $kR > 1$  for most of the time.

In Fig. 1, we show the dynamics of the aggregation upon addition of increasing amounts of pyridine. Adding a very small amount of pyridine ( $10^{-5}$  M) results in an extremely slow aggregation process (Fig. 1, curve *a*), with a dependence on time,  $t$ , reasonably well described by  $R = R_0 e^{Ct}$ , where  $C$  depends on the experimental conditions. In contrast, if a much larger amount of pyridine is added ( $10^{-2}$  M), the resulting aggregation is much faster, and the dynamics are characteristic of diffusion-limited aggregation,<sup>9</sup> with  $R \sim t^{1/d_f}$  (Fig. 1, curve *c*). Addition of an intermediate amount of pyridine ( $10^{-4}$  M) results in a crossover behavior, with an initially slow, exponential dynamics, which ultimately crosses over to exhibit the behavior characteristic of diffusion-limited aggregation (Fig. 1, curve *b*). The inset in Fig. 1 highlights the different initial rates of aggregation. We emphasize that the behavior illustrated in Fig. 1 is quite universal, and the

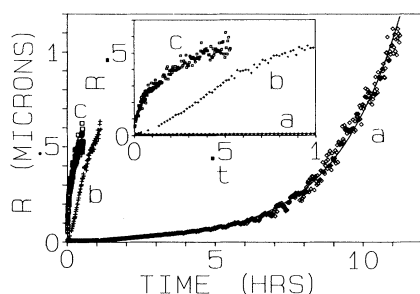


FIG. 1. Increase of characteristic cluster size with time for (curve *a*) reaction-limited, (curve *b*) crossover, and (curve *c*) diffusion-limited kinetics. The inset shows the initial behavior on an expanded scale. The reaction-limited dynamics are fitted by  $R = 0.0079e^{t/2.24}$ , where  $R$  is in microns and  $t$  in hours. For clarity, the initial concentration used to obtain curve *b* was one-half of that used for curves *a* and *c*.

dynamics are always describable by one of these classes.

The rapid and slow regimes of kinetic aggregation are also characterized by markedly different properties of the resultant aggregates. Figure 2(a) shows transmission electron microscope (TEM) pictures of a typical cluster aggregated under diffusion-limited conditions, and Fig. 2(b) shows one aggregated under the slow aggregation conditions. Each aggregate has a mass of about 5000 gold particles, but their structure and characteristic size are clearly different. For the diffusion-limited case, TEM analysis<sup>4</sup> of both the cluster-to-cluster variation of the mass as a function of the radius, as well as the internal mass correlations within a single cluster, has shown that the aggregates are fractals with  $d_f = 1.75 \pm 0.05$ . In contrast, the clusters produced with slow aggregation result in TEM images that have a substantially higher density, with many regions of overlapping particles. Thus a measure of  $d_f$  by analysis of the internal mass correlations within the cluster does not give meaningful results. Nevertheless, we do have sufficient dynamic range in the gray scales of the photographs to resolve individual gold particles to a thickness of roughly three deep. Thus we are still able to obtain an accurate measure of the mass of the clusters as a function of their radius, and we find that the clusters produced by the slow aggregation also show a scaling behavior of the cluster-to-cluster variation of their mass as a function of their radius,  $M \sim R^{d_f}$ , as expected for a fractal. However, in this case, we measure  $d_f = 2.01 \pm 0.10$ .

From the analysis of the TEM images, we also obtain an approximate measure of the cluster number distribution,  $N(M)$ , defined as the number of clusters of mass  $M$ . We find a different behavior for each type of aggregation,<sup>11</sup> which is best evidenced in the forms of the mass-weighted cluster distribution,  $MN(M)$ .

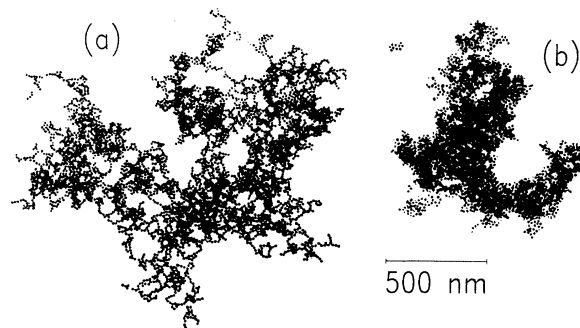


FIG. 2. Transmission electron micrographs of clusters aggregated by use of (a) diffusion-limited kinetics and (b) reaction-limited kinetics.

For the diffusion-limited aggregation,  $MN(M)$  exhibits a well defined peak whose mass increases in time. In contrast, for the slow aggregation, the behavior of  $MN(M)$  appears to be best characterized as a power law, which results in  $N(M) \sim M^{-\tau}$ , with  $\tau = 1.5 \pm 0.3$ .

To obtain a better estimate of the internal mass correlations of both classes of aggregates, we also determined  $d_f$  from the light scattering structure factor, which for a fractal exhibits scaling behavior<sup>5,13</sup>  $S(k) \sim k^{-d_f}$  for  $a \ll k^{-1} \ll R$ . While the shape of  $S(k)$  evolves in time at the early stages of the aggregation, once the dynamic light scattering measurements show that  $R > k^{-1}$  for all  $k$  used,  $S(k)$  remains constant in time. In Fig. 3, we show  $S(k)$  both for the case of diffusion-limited aggregation, curve *a*, and for the case of the slow aggregation conditions, curve *b*. The data are both well described by power laws, expected for a fractal. For the diffusion-limited aggregation, we measure  $d_f = 1.77 \pm 0.05$ , while for the slow aggregation, we measured  $d_f = 2.05 \pm 0.05$ . The slight deviation from the power-law behavior observed at higher  $k$  is attributed to the optical absorption of the colloid and is reduced at lower colloid concentrations.

There are two important questions about the suitability of light scattering that must be addressed. The

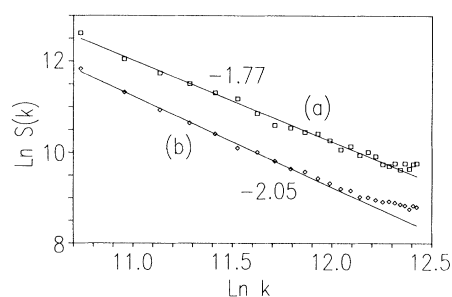


FIG. 3. Logarithmic plot of  $S(k)$  for clusters aggregated with (curve *a*) diffusion-limited kinetics and (curve *b*) reaction-limited kinetics. The fractal dimensions are (curve *a*) 1.77 and (curve *b*) 2.05. The units of  $k$  are  $\mu\text{m}^{-1}$ .

first is whether polydispersity<sup>12</sup> affects the exponent observed for  $S(k)$ . For diffusion-limited dynamics, where  $MN(M)$  exhibits a well defined peak, this will not occur once  $kR > 1$ . Similarly, for the power-law distribution obtained for slow aggregation, the scattered intensity at any  $k$  will be dominated by the contributions of the largest clusters that  $\tau < 2$  and  $kR > 1$  for these large clusters. A second problem is whether the Born approximation for weak scattering,<sup>10</sup> which is implicit in our interpretation of  $S(k)$ , is really satisfied for the gold clusters. For the aggregated colloids, we measure the integrated scattering, to within 3° of the forward direction, to be  $\leq 1\%$  of the light incident on the cross-sectional area of a typical cluster. Thus the scattering is sufficiently weak so that multiple scattering is not a problem. We note that this is an important feature of the light scattering from these gold clusters and is due to the very tenuous nature of their fractal structures. We conclude, therefore, that the measured  $S(k)$  does give an accurate determination of  $d_f$ .

The origin of the kinetic behavior in the slow regime can be understood by consideration of the nature of the short-range interaction energy between two approaching particles. This can be discussed within the Derjaguin-Landau-Verwey-Overbeek model,<sup>14</sup> which consists of a screened Coulombic repulsive barrier, with a height  $E_b$ , determined by the surface charge, and a screening length,  $l_s$ , determined by the ion concentration in solution. The likelihood of two particles sticking upon approach to within  $l_s$  is  $\gamma \sim e^{-E_b/k_b T}$ . However, the energies of the bonds formed upon sticking are  $\gg k_b T$ , since the growth is irreversible. Initially,  $E_b \gg k_b T$  and  $l_s \sim 10$  nm and the colloid does not aggregate. Pyridine displaces the charged ions adsorbed on the colloid surface, without significantly changing the ionic concentration in solution. This reduces  $E_b$  without affecting  $l_s$ , and therefore directly affects the sticking probability. Addition of sufficient pyridine displaces nearly all the charge so that  $E_b \ll k_b T$  and results in diffusion-limited aggregation. However, addition of less pyridine causes only a small amount of the charge to be displaced, so that  $E_b \geq k_b T$ , and  $\gamma \ll 1$ . In the slow regime, we find a very sensitive dependence of the initial rate of aggregation,  $C$ , on the concentration of pyridine added. This is consistent with  $C$  being dependent on  $\gamma$  and hence exponentially dependent on the pyridine concentration. This dependence is further borne out by the temperature dependence of the aggregation rate. If the surface coverage of pyridine is maintained constant, we find a temperature dependence consistent with  $C$  being proportional to  $e^{-E_b/k_b T}$ . Therefore, we conclude that the kinetics are limited by the sticking probability, rather than by diffusion, and the slow aggregation regime is labeled reaction-limited kinetics.

The origin of the properties of the clusters produced

in the reaction-limited regime can now be understood as well. Since the probability of sticking is so low, the aggregating clusters will have the opportunity to explore a large number of possible mutual configurations, which leads to some interpenetration, and therefore denser aggregates. In contrast, in diffusion-limited aggregation, the interior of the clusters is screened from penetration,<sup>15</sup> which results in a more tenuous structure. However, in both regimes, once a bond is formed, it is so strong that the aggregation is still an irreversible, kinetic process and the resultant structures are still fractals. These regimes can thus be viewed as cluster-cluster aggregation with different trajectory dimensions,<sup>16</sup>  $d_t$ . For diffusion-limited aggregation,  $d_t = 2$  and  $d_f = 1.75 \pm 0.05$ , while for reaction-limited aggregation,  $d_t = 0$  and  $d_f = 2.05 \pm 0.05$ . The divergence of the aggregation rate for the reaction-limited dynamics, which occurs at large  $t$ , reflects the fact that larger clusters, with their greater exposed contact area, have a greater probability of sticking. This also accounts for the behavior of  $N(M)$ , since the small aggregates have a much lower likelihood of sticking, and therefore are left behind in the aggregation process. Of course, ultimately both the concentration of clusters, as well as their diffusion constants, decrease, so that diffusion plays an increasingly important role in limiting the kinetics, and the aggregation crosses over to diffusion-limited. Indeed, we find experimentally that this crossover occurs when the aggregation rate,  $dR/dt$ , measured for the reaction-limited dynamics, becomes comparable to the rate measured for purely diffusion-limited dynamics at the same characteristic cluster concentration.

Our observations of the behavior of the reaction-limited kinetic aggregation are in good agreement with recent theoretical work. A computer simulation of reaction-limited kinetics<sup>17,18</sup> has obtained  $d_f = 2.0$ , in good agreement with our measurement. In addition, Ball *et al.*<sup>16</sup> have shown that the dynamics of reaction-limited aggregation depend very sensitively on the structure of the aggregates. When  $d_f \geq 2$ , they are able to account for both the exponential dynamics and the form of  $N(M)$  observed in our experiments.

Our observations may also account for the values of  $d_f$  measured for other aqueous colloids. Schaefer *et al.*<sup>5</sup> measured  $d_f = 2.12$  for the aggregation of aqueous colloidal silica particles, while Benedek<sup>6</sup> has estimated  $d_f = 2.0$  for the chemically induced and hence reaction-limited aggregation of polystyrene latex spheres. Both values are larger than the  $d_f = 1.75$  reported for diffusion-limited aggregation of gold colloids.<sup>4</sup> However, in both cases, the aggregation is irreversible, and may be best described by reaction-limited kinetics; this could account for the reported values of  $d_f$ . This results in a unified picture of all aqueous systems measured to date, wherein the values

of  $d_f$  depend on the kinetic regime of the aggregation.

In conclusion, our results show that the variation in the short-range forces between the individual particles does play an important role in the determination of the long-range dilation symmetry of the resultant aggregates. When  $E_b \ll k_b T$ , the kinetics are diffusion-limited, can be modeled with  $d_t = 2$ , and result in aggregates with  $d_f = 1.75 \pm 0.05$ . In contrast, when  $E_b \geq k_b T$ , the kinetics are reaction-limited, can be modeled with  $d_t = 0$ , and result in aggregates with  $d_f = 2.05 \pm 0.05$ . While our results are obtained for gold colloids, we expect similar behavior for the aggregation of many other systems. The key criteria inherent in our picture are that the aggregation be irreversible with little subsequent reorganization of the cluster structure, that the actual cluster motion be diffusive, and that it be homogeneous, cluster-cluster aggregation. These will be achieved when the interparticle potential can be described by the Derjaguin-Landau-Verwey-Overbeek model, and the aggregation is into the primary minimum.<sup>14</sup> Then these values of  $E_b$  represent the limiting forms of the interparticle potential that can result in aggregation. In addition, these values of  $d_t$  represent the limits of the physically realizable trajectory dimensions. This strongly suggests that, for the gold and similar colloid systems, the limiting values of the fractal dimension of the clusters formed by kinetic, irreversible cluster-cluster colloid aggregation are  $1.75 \leq d_f \leq 2.05 (\pm 0.05)$ .

We thank Tom Witten and Robin Hall for many enlightening discussions, and Richard Stephens for the scattering cross-section measurements.

<sup>(a)</sup>Also at Department of Physics, City College of New York, New York, N.Y. 10031.

<sup>1</sup>*Kinetics of Aggregation and Gelation*, edited by F. Family and D. P. Landau (North-Holland, Amsterdam, 1984).

<sup>2</sup>P. Meakin, Phys. Rev. Lett. **51**, 1119 (1983).

<sup>3</sup>M. Kolb, R. Botet, and R. Jullien, Phys. Rev. Lett. **51**, 1123 (1983).

<sup>4</sup>D. A. Weitz and M. Oliveria, Phys. Rev. Lett. **52**, 1433 (1984).

<sup>5</sup>D. W. Schaefer, J. E. Martin, P. Wiltzius, and D. S. Cannell, Phys. Rev. Lett. **52**, 2371 (1984).

<sup>6</sup>D. Johnston and G. Benedek, in Ref. 1, p. 181.

<sup>7</sup>B. V. Enustun and J. Turkevitch, J. Am. Chem. Soc. **85**, 3317 (1963).

<sup>8</sup>D. A. Weitz and J. S. Huang, in Ref. 1, p. 19.

<sup>9</sup>D. A. Weitz, J. S. Huang, M. Y. Lin, and J. Sung, Phys. Rev. Lett. **53**, 1657 (1984).

<sup>10</sup>B. J. Berne and R. Pecora, *Dynamic Light Scattering* (Wiley, New York, 1976).

<sup>11</sup>D. A. Weitz, M. Y. Lin, and J. S. Huang, to be published.

<sup>12</sup>J. E. Martin and B. J. Ackerson, to be published.

<sup>13</sup>S. K. Sinha, T. Freltoft, and J. Kjems, in Ref. 1, p. 87.

<sup>14</sup>E. J. W. Verwey and J. Th. G. Overbeek, *Theory of the Stability of Lyophobic Colloids* (Elsevier, New York, 1948).

<sup>15</sup>T. A. Witten, Jr. and L. M. Sander, Phys. Rev. Lett. **47**, 1400 (1981).

<sup>16</sup>R. C. Ball, D. A. Weitz, T. A. Witten, and F. Levraz, to be published.

<sup>17</sup>R. Jullien, M. Kolb, and R. Botet, J. Phys. (Paris), Lett. **45**, L211 (1984).

<sup>18</sup>M. Kolb and R. Jullien, J. Phys. (Paris), Lett. **45**, L977 (1984).